Applied and Environmental Microbiology

Novel Mono-, Di-, and Trimethylornithine Membrane Lipids in Northern Wetland Planctomycetes

Eli K. Moore, Ellen C. Hopmans, W. Irene C. Rijpstra, Laura Villanueva, Svetlana N. Dedysh, Irina S. Kulichevskaya, Hans Wienk, Frans Schoutsen and Jaap S. Sinninghe Damsté

Appl. Environ. Microbiol. **2013, 79(22):6874. DOI: 10.1128/AEM.02169-13.**
Published Ahead of Print 30 August 2013.

AEM
Journals.ASM.org

Novel Mono-, Di-, and Trimethylornithine Membrane Lipids in Northern Wetland Planctomycetes

Eli K. Moore,[a] Ellen C. Hopmans,[a] W. Irene C. Rijpstra,[a] Laura Villanueva,[a] Svetlana N. Dedysh,[b] Irina S. Kulichevskaya,[b] Hans Wienk,[c] Frans Schoutsen,[d] Jaap S. Sinninghe Damsté[a]

Royal Netherlands Institute for Sea Research, Department of Marine Organic Biogeochemistry, Texel, The Netherlands[a]; S. N. Winogradsky Institute of Microbiology, Russian Academy of Sciences, Moscow, Russia[b]; Bijvoet Center for Biomolecular Research, Utrecht University, Utrecht, The Netherlands[c]; Thermo Fisher Scientific, Breda, The Netherlands[d]

Northern peatlands represent a significant global carbon store and commonly originate from *Sphagnum* moss-dominated wetlands. These ombrotrophic ecosystems are rain fed, resulting in nutrient-poor, acidic conditions. Members of the bacterial phylum *Planctomycetes* are highly abundant and appear to play an important role in the decomposition of *Sphagnum*-derived litter in these ecosystems. High-performance liquid chromatography coupled to high-resolution accurate-mass mass spectrometry (HPLC-HRAM/MS) analysis of lipid extracts of four isolated planctomycetes from wetlands of European north Russia revealed novel ornithine membrane lipids (OLs) that are mono-, di-, and trimethylated at the ε-nitrogen position of the ornithine head group. Nuclear magnetic resonance (NMR) analysis of the isolated trimethylornithine lipid confirmed the structural identification. Similar fatty acid distributions between mono-, di-, and trimethylornithine lipids suggest that the three lipid classes are biosynthetically linked, as in the sequential methylation of the terminal nitrogen in phosphatidylethanolamine to produce phosphatidylcholine. The mono-, di-, and trimethylornithine lipids described here represent the first report of methylation of the ornithine head groups in biological membranes. Various bacteria are known to produce OLs under phosphorus limitation or fatty-acid-hydroxylated OLs under thermal or acid stress. The sequential methylation of OLs, leading to a charged choline-like moiety in the trimethylornithine lipid head group, may be an adaptation to provide membrane stability under acidic conditions without the use of scarce phosphate in nutrient-poor ombrotrophic wetlands.

Northern peatlands are a significant global carbon store, accounting for approximately one-third of global soil organic carbon, despite making up only 3% of the world's land area (1–3). Areas with peatland development correspond closely to the distribution of *Sphagnum* moss-dominated bogs (4). The ombrotrophic, nutrient-poor, acidic conditions of these wetlands, along with low temperatures and the presence of decay-resistant phenolic compounds and waxes in *Sphagnum* tissues, lead to low decomposition rates of *Sphagnum*-derived litter (5–9). Consequently, carbon sequestration due to net primary production in *Sphagnum*-dominated bogs is greater than the amount of carbon lost to the atmosphere by decomposition of dead organic matter, making northern wetlands an important global carbon sink (10–12).

The composition of the bacterial community in *Sphagnum* peat bogs is fundamentally different from that of the community that decomposes plant debris in eutrophic systems at neutral pH (13–15). It has been recently discovered that *Planctomycetes* make up an important part of the bacterial population responsible for *Sphagnum* decomposition, accounting for up to 14% of total bacterial cells (14, 16, 17). Cell numbers of planctomycetes have been observed to increase in the late stages of *Sphagnum* debris degradation (14). All currently described peat-inhabiting planctomycetes are capable of degrading various heteropolysaccharides, while only one of them, *Telmatocola sphagniphila*, possesses weak cellulolytic potential (18–22). The addition of available nitrogen to cellulose-amended *Sphagnum* peat degradation experiments resulted in a decrease of the relative abundance of *Planctomycetes* in the total microbial community (15). This suggests that planctomycetes in ombrotrophic wetlands are highly adapted to nutrient-poor conditions and contribute mainly to the final stages of plant litter decomposition.

Various studies have predicted that northern peatlands will change from an atmospheric carbon sink to a source in future climate-warming scenarios, further accelerating global warming (23, 24). High temperature sensitivity of soil respiration at low temperatures (25, 26) makes these ecosystems especially susceptible to climate impacts. It has been observed that a 1°C temperature increase in *in situ* subarctic peatland climate manipulation experiments accelerated total ecosystem respiration rates by 50 to 60%, depending on the season (27). Heterotroph-dominated subsurface peat respiration accounted for at least 70% of the increased respiration rates, demonstrating that climate change may have a major impact on the microbial recycling of stored organic carbon in northern wetlands. Therefore, it is important to study the microbial communities involved in the degradation of *Sphagnum*-derived material and the mechanisms of their adaptation to ombrotrophic conditions, including *Planctomycetes*, of which little is known.

Cell membranes are built out of intact polar lipids (IPLs), which consist of a polar head group connected to hydrophobic carbon chain tail groups. IPLs can be useful biomarker molecules, because their molecular structures can be taxonomically and environmentally specific and are thought to represent living biomass (28, 29). Given the

Received 1 July 2013 **Accepted** 23 August 2013
Published ahead of print 30 August 2013
Address correspondence to Eli K. Moore, Elisha.Moore@nioz.nl.
Supplemental material for this article may be found at http://dx.doi.org/10.1128/AEM.02169-13.

doi:10.1128/AEM.02169-13

unique environmental niche that these *Sphagnum* bog *Planctomycetes* occupy, their membranes may be adapted to these conditions and may contain unique biomarker lipids that could be used to further investigate the role of *Planctomycetes* in this globally important ecosystem and to indicate how they may respond to environmental change. Indeed, all planctomycete strains that have been isolated from *Sphagnum* wetlands of northern Russia contained polar membrane lipids with unknown structures (19, 21, 22) that might have biomarker potential. Here, we describe the isolation and characterization of several of these unidentified polar membrane lipids. High-resolution accurate-mass orbitrap mass spectrometry (HRAM/OT/MS) combined with nuclear magnetic resonance (NMR) revealed a series of ornithine lipids with increasing head group methylation. These lipids appear to be common in planctomycetes from this unique environment.

MATERIALS AND METHODS

Strains and culture conditions. The planctomycetes *Singulisphaera acidiphila* MOB10^T (DSM 18658^T), *Singulisphaera rosea* S26^T (DSM 23044^T), *T. sphagniphila* SP2^T and OB3 (DSM 23888^T), and *Gemmata*-like strain SP5 were isolated from the upper oxic layer (0 to 10 cm) of acidic peat collected from wetlands of European north Russia and described by Kulichevskaya et al. (19, 21, 22; see Table S1 in the supplemental material). *S. acidiphila* MOB10^T and *S. rosea* S26^T were grown in M31 liquid medium (a modification of medium 31 described by Staley et al. [30] containing [per liter of distilled water] KH_2PO_4, 0.1 g; Hutner's basal salts, 20 ml; *N*-acetylglucosamine, 1.0 g; peptone, 0.1 g; yeast extract, 0.1 g; pH 5.8). *T. sphagniphila* SP2^T and OB3, as well as *Gemmata*-like strain SP5, were grown in liquid medium M1 with the following composition (per liter of distilled water): KH_2PO_4, 0.1 g; $(NH_4)_2SO_4$, 0.1 g; $MgSO_4 \cdot 7H_2O$, 0.1 g; $CaCl_2 \cdot 2H_2O$, 0.02 g; yeast extract, 0.1 g; glucose, 0.25 g; 1 ml of trace element solution 44; and 1 ml Staley's vitamin solution (30); pH 5.5. Cultivation was done in 500-ml flasks containing 100 ml medium. Cultures were incubated at 22°C on a shaker and harvested in the late exponential growth phase. Biomass was collected and freeze-dried for extraction and analysis.

Lipid extraction. Lipids were extracted from the freeze-dried biomass of each culture by a modified Bligh and Dyer method (31). For structural comparison, lipids were also extracted from freeze-dried biomass of the bacteriodete *Flavobacterium johnsoniae*, known to contain a high concentration of ornithine lipids. The freeze-dried biomass of each culture was fully submerged and extracted three times in methanol-dichloromethane-phosphate (MeOH-DCM-P) buffer (2:1:0.8 [vol/vol/vol]) extraction solvent for 10 min in an ultrasonic bath (P buffer; 8.7 g K_2PO_4 liter^{-1} bidistilled water adjusted to pH 7 to 8 with 1 N HCl). Extracts were centrifuged for 2 min at 1,400 × *g* to separate the DCM phase from the MeOH-P buffer phase, and the lower DCM layer was pipetted into a separate vial. The MeOH-P buffer layer was washed twice more with DCM and centrifuged, and the resulting DCM layers were pipetted into the same vial as the original DCM layer. DCM was removed under a stream of nitrogen, and the residue was dissolved in injection solvent (hexane–2-propanol–H_2O; 718:271:10 [vol/vol/vol]) and filtered through a 0.45-μm, 4-mm-diameter True Regenerated Cellulose syringe filter (Grace Davison) prior to injection. Extracts were stored at −80°C until analysis.

HPLC-MS analysis. Intact polar lipids were analyzed by high-performance liquid chromatography–electrospray ionization–ion trap mass spectrometry (HPLC-ESI/IT/MS) according to the method of Sturt et al. (28) with some modifications (32). Briefly, an Agilent 1200 series high-performance liquid chromatograph with a thermostated autoinjector was coupled to a Thermo LTQ XL linear ion trap mass spectrometer with an Ion Max source and ESI probe (Thermo Scientific, Waltham, MA). The typical lipid extract injection concentration was 2 mg/ml, and the injection volume was 10 μl. Chromatographic separation was performed on a Lichrosphere diol column (250 mm by 2.1 mm; 5-μm particles; Grace Alltech Associates Inc.). Elution was achieved with hexane–2-propanol–formic acid–14.8 M aqueous NH_3 (79:20:0.12:0.04 [vol/vol/vol/vol]) (A) and 2-propanol–water–formic acid–14.8 M aqueous NH_3 (88:10:0.12:0.04 [vol/vol/vol/vol]) (B) starting at 10% B, followed by a linear increase to 30% B in 10 min, followed by a 20-min hold and a further increase to 65% B at 45 min. The flow rate was 0.2 ml min^{-1}, and the total run time was 60 min, followed by a 20-min reequilibration period. The lipid extracts were analyzed by scanning a mass range of *m/z* 400 to 2,000 in positive-ion mode, followed by data-dependent, dual-stage tandem MS (MS^2), in which the four most abundant masses in the mass spectrum were fragmented successively (normalized collision energy, 25; isolation width, 5.0; activation Q, 0.175). Each MS^2 was followed by data-dependent, triple-stage tandem MS (MS^3), where the base peak of the MS^2 spectrum was fragmented under fragmentation conditions identical to those described for MS^2. The ion trap MS was calibrated using the Thermo Scientific LTQ ESI Positive Ion Calibration Solution (containing a mixture of caffeine, methionine-arginine-phenylalanine-alanine (MRFA), and Ultramark 1621 in an acetonitrile-methanol-acetic solution). The performance of HPLC-ESI/IT/MS was monitored by regular injections of platelet-activating factor (PAF) standard (1-*O*-hexadecyl-2-acetyl-*sn*-glycero-3-phosphocholine). Relative differences in ornithine and methylornithine IPL ionization and instrument response were corrected for by the use of external standards (Avanti Polar Lipids, Inc.; 1,2-dipalmitoyl-*sn*-glycero-3-phosphoethanolamine, 1,2-dipalmitoyl-*sn*-glycero-3-phosphoethanolamine-*N*-methyl, 1,2-dipalmitoyl-*sn*-glycero-3-phosphoethanolamine-*N*,*N*-dimethyl, and 1,2-dipalmitoyl-*sn*-glycero-3-phosphocholine).

HPLC-HRAM/OT/MS analysis of the *T. sphagniphila* extract was accomplished on a 3000 UltiMate series liquid chromatograph with a thermostated autoinjector coupled to a Q Exactive high-resolution accurate-mass orbitrap mass spectrometer (Thermo Scientific). The chromatographic conditions and column were the same as those described above for HPLC-ESI/IT/MS. The positive-ion ESI settings were as follows: capillary temperature, 275°C; sheath gas (N_2) pressure, 35 arbitrary units (AU); auxiliary gas (N_2) pressure, 10 AU; spray voltage, 4.0 kV; probe heater temperature, 300°C; S-lens, 50 V. Target lipids were analyzed with a mass range of *m/z* 400 to 1,000 (resolution, 70,000), followed by data-dependent MS^2 (resolution, 17,500), in which the five most abundant masses in the mass spectrum were fragmented successively (normalized collision energy, 35; isolation width, 1.0). The Q Exactive was calibrated within a mass accuracy range of 1 ppm using the Thermo Scientific Pierce LTQ Velos ESI Positive Ion Calibration Solution (containing a mixture of caffeine, MRFA, Ultramark 1621, and *N*-butylamine in an acetonitrile-methanol-acetic solution).

Fatty acid analysis. An aliquot of *T. sphagniphila* Bligh and Dyer extract was hydrolyzed with 1.5 N HCl in MeOH by reflux for 3 h. The hydrolysate was adjusted to pH 4 with 2 N KOH-MeOH (1:1 [vol/vol]). Water was added to give a final ratio of 1:1 H_2O-MeOH and then extracted three times with DCM. The DCM fractions were collected and dried over sodium sulfate. The extract was then methylated with diazomethane (33), followed by silylation in pyridine with *N*,*O*-bis(trimethylsilyl)trifluoro-acetamide (BSTFA) at 60°C for 20 min. The methylated-silylated extracts were then dissolved in ethyl acetate for gas chromatography (GC)-MS analysis.

GC and GC-MS. GC was performed using a Hewlett-Packard gas chromatograph (HP6890) equipped with an on-column injector and a flame ionization detector. Chromatography was accomplished using a fused-silica capillary column (25 m by 0.32 mm) coated with CP Sil-5 CB (film thickness, 0.12 μm) with helium as the carrier gas. The samples were injected at 70°C, and the oven temperature was ramped to 130°C at 20°C/min and then 4°C/min to 320°C, where it was held for 10 min. GC-MS was performed on a Finnigan Trace Ultra gas chromatograph interfaced with a Finnigan Trace DSQ mass spectrometer operated at 70 eV with a mass range of *m/z* 40 to 800 and a cycle time of 1.7 s (resolution, 1,000). The gas chromatograph employed a fused-silica capillary column as described for GC and also used helium as the carrier gas. The same temperature program was used as with GC.

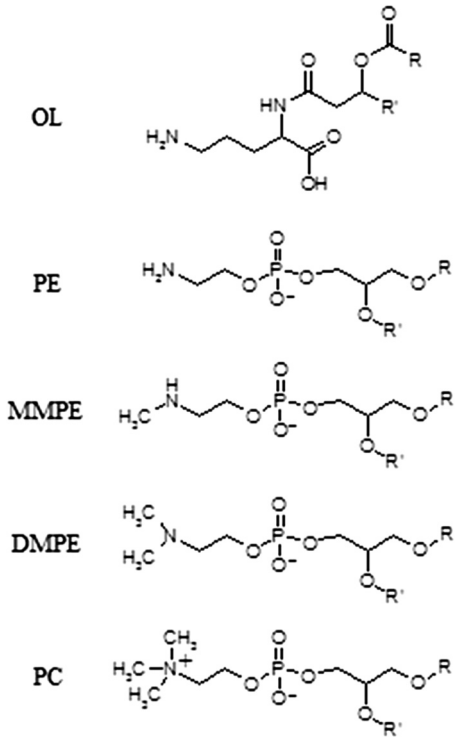

FIG 1 Molecular structures of OL, PE, MMPE, DMPE, and PC.

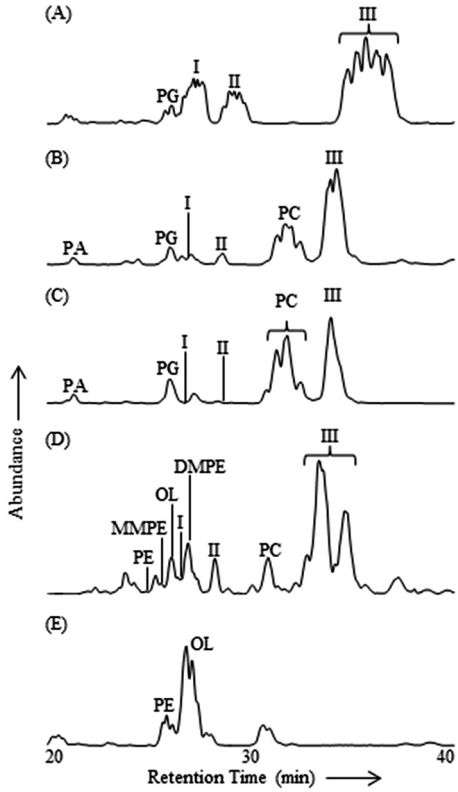

FIG 2 HPLC-ESI/IT/MS base peak chromatograms (*m/z* 400 to 2,000) of Bligh and Dyer lipid extracts from planctomycete cultures. (A) *T. sphagniphila*. (B) *S. rosea*. (C) *S. acidiphila*. (D) *Gemmata*-like strain SP5. (E) *F. johnsoniae* (bacteriodete).

Target lipid isolation. Target lipids were isolated from extracts using an Agilent Technologies (Santa Clara, CA) 1100 series LC, equipped with an autoinjector, and a fraction collector (Foxy Jr.; Isco, Inc., Lincoln, NE). A first isolation was achieved on a semipreparative Lichrosphere diol column (10 by 250 mm; 5 μm; Grace Alltech Associates Inc.) according to the method of Boumann et al. (34) with the same gradient program described above for HPLC-ESI/IT/MS, but at a flow rate of 3 ml min^{-1}. The typical injection volume was 200 μl, containing up to 2 mg material. Column effluent was collected in 1-min fractions, which were screened for the presence of target lipids by flow injection analysis using the method of Smittenberg et al. (35) with ESI/IT/MS (5-μl injection of each fraction; ESI source settings were same as those described above for HPLC-ESI/IT/MS with a scan range of *m/z* 400 to 2,000). Fractions containing target lipids were pooled and further purified on a second Lichrosphere diol column (4.6 by 250 mm; 5 μm; Grace Alltech Associates Inc.). The typical injection volume was 65 μl, containing up to 0.65 mg of material. Lipids were eluted using a gradient program and conditions identical to those described above for HPLC-ESI/IT/MS (but with slightly modified mobile phases so that neither mobile phase A nor B contained NH_3 or formic acid) at a flow rate of 1 ml min^{-1}. Column effluent was collected in 15-s fractions and screened as described above. Fractions containing target lipids were again combined, and the elution solvent was removed under a stream of nitrogen. Purity was assessed by HPLC-ESI/IT/MS as described above for IPL analysis. The isolated lipids were stored at −80°C prior to further analysis.

Nuclear magnetic resonance. The purified lipids were dissolved in 99.9% $CDCl_3$ at a concentration of 1.5 μmol ml^{-1}, and NMR experiments were performed at 298 K on Bruker 600-MHz and 750-MHz Avance spectrometers equipped with triple-resonance TXI probes and running under TOPSPIN 2.1. The 600-MHz one-dimensional (1D) ^{1}H and ^{1}H-decoupled 1D ^{13}C and DEPT-135 experiments were recorded with spectral widths/offsets of 24 ppm/6 ppm, 200 ppm/100 ppm, and 200 ppm/100 ppm and with 16,384 (16k), 1,024 (1k), and 1,024 (1k) complex points, respectively. The 14- by 14-ppm 2D correlation spectroscopy (COSY), total correlation spectroscopy (TOCSY), and nuclear Overhauser effect spectroscopy (NOESY) experiments were performed at 750 MHz with 512 by 512 complex points and an offset frequency of 6 ppm. Mixing times were 60 ms and 250 ms for TOCSY and NOESY, respectively. The (^{1}H, ^{13}C)-heteronuclear single-quantum correlation spectroscopy (HSQC) and (^{1}H, ^{13}C)-heteronuclear multiple-bond correlation spectroscopy (HMBC) experiments were recorded at 600 MHz with spectral widths/offsets of 14/6 ppm for protons and 200/100 ppm for carbon-13. Spectra were calibrated with respect to internal residually protonated $CHCl_3$ at 7.24 ppm (^{1}H) and 77.0 ppm (^{13}C).

RESULTS

Unknown IPLs detected by HPLC-ESI/IT/MS. Intact polar lipid analysis of four recently described planctomycete strains from Russian peatlands revealed known and unknown membrane lipid structures. In addition to the commonly observed lipid classes phosphatidylcholine (PC), phosphatidylglycerol (PG), phosphatidic acid (PA), phosphatidylethanolamine (PE), monomethylphosphatidylethanolamine (MMPE), dimethylphosphatidylethanolamine (DMPE), and amino acid-containing ornithine lipids (OLs) (phosphorus-free membrane lipids found only in bacteria) (Fig. 1), three groups of unknown lipids (I to III) were observed in the lipid extracts from each of the four analyzed planctomycete species by HPLC-ESI/IT/MS polar lipid analysis, in agreement with results previously reported by Kulichevskaya et al. (19, 21, 22) (Fig. 2). Group I, II, and III lipids made up the majority of IPLs in *T. sphagniphila* and *Gemmata*-like SP5 extracts and a large portion of the IPLs in *S. rosea* and *S. acidiphila* (Table 1). The lipid

TABLE 1 Contributions of group I, II, and III lipids to the total lipid signal[a]

Species/strain	Contribution (%)		
	I	II	III
T. sphagniphila	24.7	13.9	45.3
S. rosea	<1.0	3.6	44.4
S. acidiphila	<1.0	<1.0	37.2
SP5	<1.0	4.8	49.9

[a] As determined from the ESI/IT/MS base peak chromatograms of *T. sphagniphila*, *S. rosea*, *S. acidiphila*, and *Gemmata*-like strain SP5 lipid extracts.

extract from *T. sphagniphila* contained the largest amount of these unknown lipids, and the identification efforts, therefore, focused on that species. In the *T. sphagniphila* extract, each of the three unknown lipid clusters showed 5 dominant mass signals separated by 14 Th. The five main observed masses in group I (*m/z* 637, 651, 665, 679, and 693) were each 14 thomson (Th) lighter than the five masses in group II (*m/z* 651, 665, 679, 693, and 707), and the masses in group II were 14 Th lighter than the masses in group III (*m/z* 665, 679, 693, 707, and 721).

Each of the unknown lipid groups displayed ornithine-like MS fragmentation but different fragmentation products. Typical ornithine lipid MS^2 fragmentation involves the loss of a water molecule and a fatty acyl chain ($R_2CH{=}C{=}O$), followed by the loss of the second fatty acid as a ketene ($R_1CH{=}C{=}C{=}O$) during MS^3 fragmentation, resulting in a diagnostic product at *m/z* 115 ($C_5H_{11}N_2O$) representing the ornithine head group (36). Ion trap fragmentation of lipid groups I, II, and III followed a similar pattern but resulted in different fragmentation products in MS^3, suggesting a general IPL structure similar to that of ornithine lipids but with a different polar head group. Compounds in group I yielded a product of *m/z* 129 after MS^3 fragmentation. Group II was characterized by multiple low-abundance MS^3 fragmentation products at *m/z* 100, 115, 144, 161, and 185. Lipids in cluster III displayed slightly different fragmentation behavior, with the apparent loss of a fatty acid, followed by the additional loss of *m/z* 59 during MS^2 fragmentation. MS^3 fragmentation of the latter fragment resulted in the apparent loss of another fatty acid, which generated an *m/z* 116 product.

HRAM/OT/MS analysis of unidentified IPL group III. The lipid extract of *T. sphagniphila* was subjected to HRAM/OT/MS analysis to elucidate the elemental compositions of the lipid head groups of the three unknown lipid clusters. Group III was the most abundant IPL and was therefore analyzed first. As was the case in IT/MS^2 fragmentation, the initial loss observed for the molecular ion of *m/z* 665.5824 from group III, the apparently most abundant unidentified IPL group in *T. sphagniphila*, is of a $C_{16:1}$ fatty acid (Fig. 3A). Subsequent loss of C_3H_9N generates *m/z* 352.2847, the base peak in the mass spectrum. The presence of C_3H_9N, potentially a trimethylated nitrogen, is a common molecular feature in other membrane lipid head groups, such as PCs and betaines. From the base peak, loss of a $C_{16:0}$ ketene results in a product at *m/z* 116.0709 with a molecular composition of $C_5H_{10}NO_2$. The observed fragmentation for group III molecular ion *m/z* 665.5824 appears to represent an ornithine-like lipid that is trimethylated on the ε-nitrogen position (Fig. 3B). This fragmentation pattern was observed for all molecular ions in group III lipids (Tables 2 and 3). Proposed gas phase fragmentation includes the formation of a cyclic head group structure after loss of a fatty acid, the trimethylated nitrogen, and a βOH fatty acid. This fragmentation is similar to the formation of the cyclic *m/z* 115

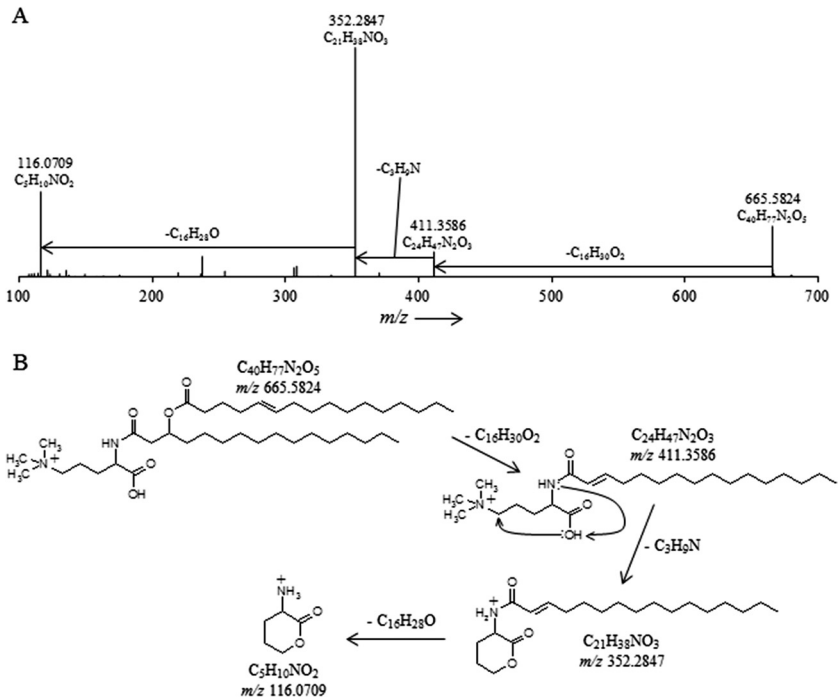

FIG 3 (A) High-resolution accurate-mass quadrupole OT/MS^2 mass spectrum of *T. sphagniphila* lipid extract group III TMO *m/z* 665.5824 ($C_{16:1}/C_{16:0}$). The chemical formulas represent neutral losses and products after MS^2 fragmentation. (B) Proposed gas phase fragmentation pathway of trimethylornithine *m/z* 665.5824.

TABLE 2 *m/z* of the molecular species, fatty acid losses, elemental compositions, and accuracy values that occur during MS fragmentation of each mass in lipid groups III, II, and I[a]

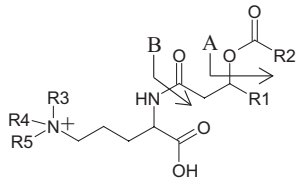

Lipid	*m/z*[b]	Rel. abun. (%)[c]	FA	Observed loss (A) (R2-COOH)	Assigned elemental composition	Accuracy (Δ mmu[d])	βOH-FA	Observed loss (B) (R1-CH=C=C=O)	Assigned elemental composition	Accuracy (Δ mmu[d])
Group III (TMO)										
$C_{40}H_{77}N_2O_5$	665	20.4	$C_{16:1}$	254.2239	$C_{16}H_{30}O_2$	0.7	$C_{16:0}$	236.2138	$C_{16}H_{28}O$	0.2
$C_{41}H_{79}N_2O_5$	679	29.3	$C_{16:1}$	254.2243	$C_{16}H_{30}O_2$	0.3	$C_{17:0}$	250.2291	$C_{17}H_{30}O$	0.6
$C_{42}H_{81}N_2O_5$	693	7.3	$C_{16:1}$	254.2252	$C_{16}H_{30}O_2$	0.6	$C_{18:0}$	264.2449	$C_{18}H_{32}O$	0.4
$C_{42}H_{81}N_2O_5$	693	9.8	$C_{18:1}$	282.2556	$C_{18}H_{34}O_2$	0.3	$C_{16:0}$	236.2137	$C_{16}H_{28}O$	0.3
$C_{43}H_{83}N_2O_5$	707	23.8	$C_{18:1}$	282.2556	$C_{18}H_{34}O_2$	0.3	$C_{17:0}$	250.2293	$C_{17}H_{30}O$	0.4
$C_{44}H_{85}N_2O_5$	721	9.6	$C_{18:1}$	282.2556	$C_{18}H_{34}O_2$	0.3	$C_{18:0}$	264.2447	$C_{18}H_{32}O$	0.6
Group II (DMO)										
$C_{39}H_{75}N_2O_5$	651	12.1	$C_{16:1}$	254.2237	$C_{16}H_{30}O_2$	0.9	$C_{16:0}$	236.2137	$C_{16}H_{28}O$	0.3
$C_{40}H_{77}N_2O_5$	665	27.2	$C_{16:1}$	254.2251	$C_{16}H_{30}O_2$	0.5	$C_{17:0}$	250.2290	$C_{17}H_{30}O$	0.7
$C_{41}H_{79}N_2O_5$	679	6.5	$C_{16:1}$	254.2244	$C_{16}H_{30}O_2$	0.2	$C_{18:0}$	264.2446	$C_{18}H_{32}O$	0.7
$C_{41}H_{79}N_2O_5$	679	14.2	$C_{18:1}$	282.2554	$C_{18}H_{34}O_2$	0.5	$C_{16:0}$	236.2137	$C_{16}H_{28}O$	0.3
$C_{42}H_{81}N_2O_5$	693	34.9	$C_{18:1}$	282.2546	$C_{18}H_{34}O_2$	1.3	$C_{17:0}$	250.2291	$C_{17}H_{30}O$	0.6
$C_{43}H_{83}N_2O_5$	707	5.1	$C_{18:1}$	282.2540	$C_{18}H_{34}O_2$	1.9	$C_{18:0}$	264.2447	$C_{18}H_{32}O$	0.6
Group I (MMO)										
$C_{38}H_{73}N_2O_5$	637	18.3	$C_{16:1}$	254.2251	$C_{16}H_{30}O_2$	0.5	$C_{16:0}$	236.2138	$C_{16}H_{28}O$	0.2
$C_{39}H_{75}N_2O_5$	651	25.0	$C_{16:1}$	254.2255	$C_{16}H_{30}O_2$	0.9	$C_{17:0}$	250.2294	$C_{17}H_{30}O$	0.3
$C_{40}H_{77}N_2O_5$	665	5.6	$C_{16:1}$	254.2261	$C_{16}H_{30}O_2$	1.5	$C_{18:0}$	264.2449	$C_{18}H_{32}O$	0.4
$C_{40}H_{77}N_2O_5$	665	11.7	$C_{18:1}$	282.2577	$C_{18}H_{34}O_2$	1.8	$C_{16:0}$	236.2138	$C_{16}H_{28}O$	0.2
$C_{41}H_{79}N_2O_5$	679	27.7	$C_{18:1}$	282.2559	$C_{18}H_{34}O_2$	>0.1	$C_{17:0}$	250.2293	$C_{17}H_{30}O$	0.4
$C_{42}H_{81}N_2O_5$	693	11.8	$C_{18:1}$	282.2567	$C_{18}H_{34}O_2$	0.8	$C_{18:0}$	264.2448	$C_{18}H_{32}O$	0.5

[a] R2-COOH and R1-CH=C=C=O losses result from fragmentation to fatty acid (FA) and βOH-FA, respectively, in the structure shown. TMO, R3 = R4 = R5 = CH_3; DMO, R3 = R4 = CH_3, R5 = H; MMO, R3 = CH_3, R4 = R5 = H.

[b] Group III, M^+; groups I and II, $[M+H]^+$.

[c] Rel. abun., relative abundance, i.e., the peak area percentage of each lipid within its respective group.

[d] In general the 0.5-Δ mmu (milli-mass unit) range was used as a measure of very high-confidence molecular formula assignments, and the 1.0-Δ mmu range was used as a measure of good-confidence molecular formula assignments (63–65).

diagnostic product, formed by loss of H_2O in the head group, observed during MS fragmentation of ornithine lipids (36). In total, there are six main lipids in group III with different fatty acid compositions (*m/z* 693 consists of two coeluting isobaric lipids), which follow the proposed fragmentation pattern for the trimethylornithine (TMO) structure (Tables 2 and 3). Analysis by GC and GC-MS of the *T. sphagniphila* extract confirmed that $C_{18:1\omega5c}$ and $C_{16:1\omega5c}$ fatty acids were the most abundant core lipids, followed by $C_{16:0}$, $C_{18:0}$, βOH-C_{16}, βOH-$C_{17:0}$, and βOH-$C_{18:0}$ fatty acids. This is in agreement with previous lipid analysis reported by Kulichevskaya et al. (22).

Structural identification of trimethylornithine lipids by NMR. *T. sphagniphila* group III lipids appeared to be the most abundant unknown lipid cluster among the four analyzed planctomycetes. This lipid cluster was purified using semipreparatory HPLC for further analysis. In addition, ornithine lipids were purified from *F. johnsoniae* (Fig. 2) to be used as a reference compound for structural comparison to the *T. sphagniphila* group III lipids. Approximately 2 mg of group III lipid was isolated from the *T. sphagniphila* lipid extract and 5 mg of ornithine lipid was isolated from *F. johnsoniae* lipid extract for NMR analysis.

The ^{1}H-NMR, COSY, and ^{13}C-NMR spectra of the purified ornithine lipid agreed well with previously reported NMR structural characterization of ornithine lipids (37, 38). There were many similarities between the ^{1}H-NMR and ^{13}C-NMR signals of the purified group III lipids and ornithine lipids, particularly for the aliphatic chains (Table 4). The main differences between the TMO lipid and ornithine ^{1}H-NMR spectra were the intense signal at 3.27 ppm in the TMO lipid spectra, the absence of an ε-NH_2 signal at 5.71 ppm, and the increase in chemical shift of the α-NH and head group δ-position signals. Both the ^{1}H-NMR and ^{13}C-NMR chemical shifts of the unknown signal (^{1}H, 3.27 ppm; ^{13}C, 54 ppm) and the head group δ-position (^{1}H, 3.70; ^{13}C, 66 ppm) in the TMO lipids match the chemical shifts of the trimethylamine [$(CH_3)_3N^+$] group and adjacent carbon position (CH_2) reported for the choline group of PC lipids in previous studies [for $(CH_3)_3N^+$, ^{1}H, 3.25, and ^{13}C, 54.2; for CH_2, ^{1}H, 3.70, and ^{13}C, 66.1 (39); for $(CH_3)_3N^+$, ^{13}C, 54.3; for CH_2, ^{13}C, 66.65 (40); for $(CH_3)_3N^+$, ^{1}H, 3.30, and ^{13}C, 54.6 (41)]. (^{1}H, ^{13}C)-HSQC analysis revealed that the apparent trimethylamine proton at 3.27 ppm was directly bound to the carbon atom at 54 ppm. The (^{1}H, ^{13}C)-HSQC analysis also showed that the head group δ-position ^{1}H chemical shift was bound to an increased ^{13}C-NMR

TABLE 3 *m/z*, HRAM/OT/MS assigned molecular formulas, elemental composition, and accuracy values of formula assignments of observed losses and products that occur during MS fragmentation (Fig. 2, 3, and 4) of each mass in lipid groups III, II, and I

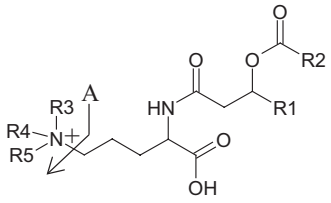

Group	*m/z*[a]	Observed loss (A)[b]	Accuracy (Δ mmu)	Observed product[c]	Accuracy (Δ mmu)	Observed product[d]	Accuracy (Δ mmu)	Observed product[e]	Accuracy (Δ mmu)	Observed product[f]	Accuracy (Δ mmu)
III (TMO)	665	59.0737	0.2	116.0710	0.2						
	679	59.0731	0.4	116.0710	0.2						
	693	59.0735	>0.1	116.0709	0.3						
	693	59.0742	0.7	116.0709	0.3						
	707	59.0739	0.4	116.0710	0.2						
	721	59.0733	0.2	116.0710	0.2						
II (DMO)	651	45.0582	0.4	116.0710	0.2	144.1020	0.5	161.1285	0.5	187.1079	0.4
	665	45.0575	0.3	116.0710	0.2	144.1020	0.5	161.1285	0.5	187.1077	0.6
	679	45.0574	0.4	116.0710	0.2	144.1021	0.4	161.1285	0.5	187.1078	0.5
	679	45.0574	0.4	116.0710	0.2	144.1021	0.4	161.1285	0.5	187.1078	0.5
	693	45.0578	>0.1	116.0710	0.2	144.1021	0.4	161.1285	0.5	187.1078	0.5
	707	45.0578	>0.1	116.0710	0.2	144.1021	0.4	161.1285	0.5	187.1078	0.5
I (MMO)	637	31.0422	>0.1	116.0710	0.2	129.1024	0.4	147.1129	0.5	173.0921	0.5
	651	31.0428	0.6	116.0710	0.2	129.1024	0.4	147.1129	0.5	173.0923	0.3
	665	31.0422	>0.1	116.0710	0.2	129.1024	0.4	147.1129	0.5	173.0922	0.4
	665	31.0417	0.5	116.0710	0.2	129.1024	0.4	147.1129	0.5	173.0922	0.4
	679	31.0427	0.5	116.0710	0.2	129.1024	0.4	147.1129	0.5	173.0923	0.3
	693	31.0422	>0.1	116.0709	0.3	129.1023	0.5	147.1128	0.6	173.0920	0.6

[a] Group III, M^+; groups I and II, $[M+H]^+$.
[b] Group III, C_3H_9N; group II, C_2H_7N; group I, CH_5N.
[c] Group III, $C_5H_{10}NO_2$; group II, $C_5H_{10}NO_2$; group I, $C_5H_{10}NO_2$.
[d] Group II, $C_7H_{14}NO_2$; group I, $C_6H_{13}N_2O$.
[e] Group II, $C_7H_{17}N_2O_2$; group I, $C_6H_{15}N_2O_2$.
[f] Group II, $C_8H_{15}N_2O_3$; group I, $C_7H_{13}N_2O_3$.

chemical shift as well compared to the head group δ-position signal in the ornithine lipid spectra.

Further confirmation of structural assignments was given by HMBC, which showed connectivity between the apparent trimethylamine signal and head group δ-position, and NOESY, which confirmed a short distance between the trimethylamine signal and head group δ-protons, as well as the other head group and fatty acid chain protons. The presence of a highly charged quaternary amine in the lipid head group explains the absence of the δ-NH_2 signal in the proton spectrum, since no protons are attached directly to the nitrogen. It may also be expected that that this functional group increases the chemical shift of the α-NH compared to the ornithine lipid, as observed. Alkene chemical shifts in the TMO NMR spectra (Table 4) were expected to be detected, as observed in the MS results. Therefore, the NMR results confirm the structural identification of the lipids in group III as a series of ornithine lipids that are trimethylated on the ε-nitrogen position (Fig. 3B and Tables 2, 3, and 4).

Structural elucidation of IPL groups II and I. The HRAM/OT/MS fragmentation of *T. sphagniphila* group II molecular ion *m/z* 651.5666 and group I *m/z* 637.5519 produced the same initial losses of a $C_{16:1}$ fatty acid observed for the TMO *m/z* 665.5824 lipid (Fig. 4 and 5 and Table 2). The group II *m/z* 379.3429 ion thus formed then loses C_2H_7N, while the group I *m/z* 383.3429 ion formed loses CH_5N (Fig. 4 and 5 and Table 3). Analogous to the loss of C_3H_9N for trimethylornithine, the loss of C_2H_7N and CH_5N appears to indicate dimethylated and monomethylated nitrogen structures, respectively (Fig. 4 and 5). After the methylated nitrogen losses, the *m/z* 352.2847 ions formed for both group II *m/z* 651.5666 and group I *m/z* 637.5519 lose a $C_{16:0}$ fatty acid, identical to what has been observed for the TMOs (Table 2), resulting in the same *m/z* 116.0710 $C_5H_{10}NO_2$ product (Table 3 and Fig. 4 and 5). For group II, fragmentation also resulted in formation of *m/z* 144.1021, *m/z* 161.1285, and *m/z* 187.1079 ions, and for group I, fragmentation resulted in *m/z* 129.1024, *m/z* 147.1129, and *m/z* 173.0921 products (Table 3 and Fig. 4 and 5). These fragmentation patterns were the same for all group II and group I lipids, respectively (Table 2).

Based on the fragmentation behavior and formula assignments of key losses and products, we propose that the unknown lipids in cluster II represent a series of ornithine lipids that are dimethylated on the ε-nitrogen position, i.e., dimethylornithine (DMO) (Fig. 4B), while unknown lipids in cluster I represent ornithine lipids that are monomethylated on the ε-nitrogen position, i.e., monomethylornithine (MMO) (Fig. 5B). As with the TMO cluster, there were five main masses in both the DMO and MMO

TABLE 4 ^{13}C- and ^{1}H-NMR signals from trimethylornithine[a] and ornithine lipids

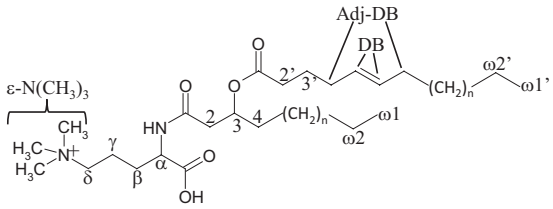

	Signal (ppm)							
	Trimethylornithine				Ornithine			
	Carbon chemical shift			Proton chemical shift	Carbon chemical shift			Proton chemical shift
Position	CH_3	CH_2	CH		CH_3	CH_2	CH	
ε-N(CH_3)$_3$		53.8		3.27				
ε-NH_2								5.71
δ		66.1		3.70		41.8		3.37
γ		19.2		1.85		21.9		1.96
β		29.9		1.95		27.9		2.62
β′		29.9		1.80		27.9		1.53
α			53.1	4.25			50.9	4.29
α-NH				7.24				6.54
2		41.9		2.50		42.0		2.51
3			71.5	5.20			71.3	5.21
4		34.8		1.58		34.1		1.62
5-ω2		29.6		1.29		29.2		1.29
ω1	22.5			0.84	22.5			0.88
2′		34.7		2.28		34.2		2.30
3′		25.1		1.58		25.1		1.62
8′-ω2		29.6		1.29		29.6		1.29
ω1′	22.5			0.84	22.5			0.88
DB		129.5		5.38				
Adj-DB		27.4		2.05				

[a] Trimethylornithine structure is shown.

clusters that represent six lipids (Tables 2 and 3). The fatty acid distributions were identical among the MMO, DMO, and TMO lipid groups, and the relative abundances of the various lipids within each group were similar (Table 2). Under the chromatographic conditions used here, the elution order of ornithine, MMO, DMO, and TMO was the same as that observed for PE, MMPE, DMPE, and PC lipids identified in the *Gemmata*-like SP5 lipid extract (Fig. 2D), displaying an increasing retention time with increasing methylation of the ε-nitrogen.

Distribution of MMO, DMO, and TMO lipids in planctomycete strains. The trimethylornithine lipids appeared to be the most abundant of the three classes of methylornithines in each of the four planctomycetes (Fig. 2). The MMO and DMO lipids were both most abundant in *T. sphagniphila*, followed by *Gemmata*-like strain SP5, *S. rosea*, and *S. acidiphila*. The dominant core lipids observed in MMOs, DMOs, and TMOs were $C_{18:1}$ and $C_{16:1}$ for *T. sphagniphila*, $C_{18:1}$ and $C_{18:0}$ for *S. rosea*, $C_{18:1}$ and $C_{18:0}$ for *S. acidiphila*, and $C_{20:1}$ and $C_{16:0}$ for the *Gemmata*-like strain SP5. This difference in fatty acid distribution observed between the lipid extracts of the four planctomycete species based on HPLC-ESI/IT/MS fragmentation among the MMO, DMO, and TMO lipids resulted in slightly different retention times of the three lipid classes for each species in the base peak chromatograms (Fig. 2).

DISCUSSION

This study describes the identification of a series of novel OLs with increasing methylation on the terminal ε-nitrogen position, resulting in mono-, di-, and trimethylated ornithine head groups. OLs are common phosphorus-free membrane lipids in bacteria but are absent in eukaryotes and archaea (42, 43). Roughly 25% of the bacteria whose genomes have been sequenced have the predicted capability to produce OLs (44). It has been proposed that OLs are important for outer membrane stability in Gram-negative bacteria due to their zwitterionic nature (45). In some bacteria OLs are produced under phosphorus limitation (46, 47) or hydroxylated under thermal or acid stress (48–50). Other amino acid-containing lipids have been identified in various bacteria, including glycine lipids (51, 52), a lysine lipid (53), and an ornithine-taurine-linked lipid (54), although they are not nearly as widespread as OLs. While the exact function of OL modifications is not yet fully described, characterization of mutants that are deficient in ornithine lipid biosynthesis and modification genes has further supported a mechanism of bacterial stress response to changing environmental conditions (44, 49, 50). The unique environmental settings from which the planctomycetes in this study were isolated and the adaptable nature of ornithine lipids in various bacteria suggest that the synthesis of methylated ornithine lipids by these microbes may be a response to the ombrotrophic conditions of northern wetlands.

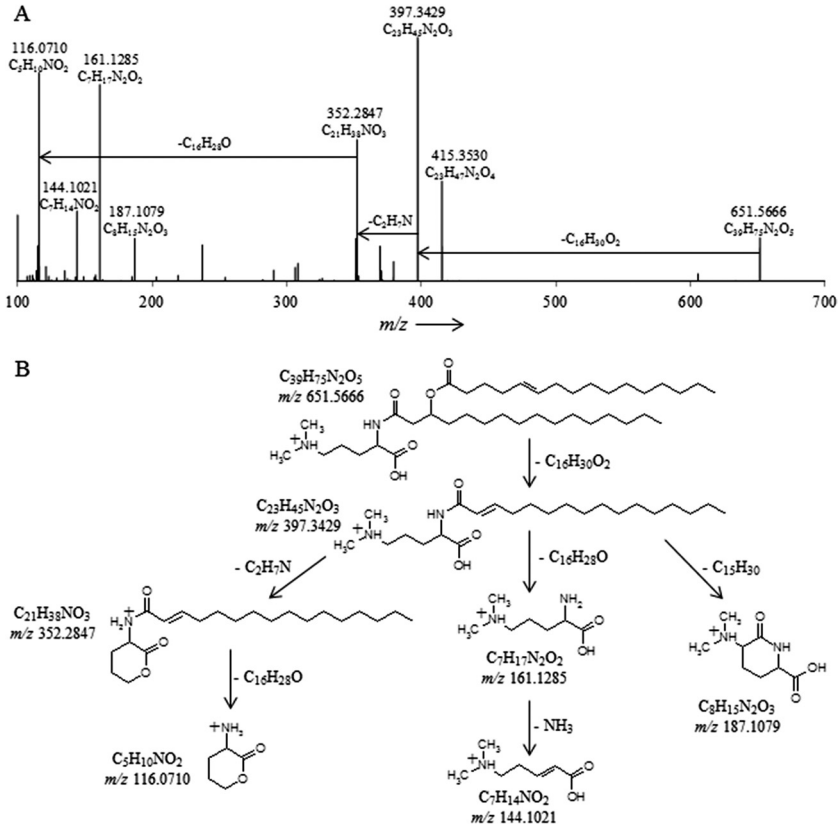

FIG 4 (A) High-resolution accurate-mass quadrupole OT/MS^2 mass spectrum of *T. sphagniphila* lipid extract group II dimethylornithine *m/z* 651.5666. The chemical formulas represent neutral losses and products after MS^2 fragmentation. (B) Proposed gas phase fragmentation pathway of dimethylornithine *m/z* 651.5666.

Increasing acidity ultimately impedes microorganism growth, causing a range of physiological problems, including outer membrane damage (55). Various microbes have developed different strategies to respond to pH stress (56–58). The hydroxylation of ornithine lipids in *Rhizobium tropici* under acidic conditions increases the potential for hydrogen bonding among individual polar lipid molecules, resulting in greater membrane stability (49, 50). Like PEs, MMPEs, DMPEs, and PCs, the addition of each subsequent methyl group to the ε-NH_2 ornithine head group in MMOs, DMOs, and TMOs appears to increase the polarity of the lipid based on LC retention time. This is especially true in the TMO lipids, where the presence of a quaternary amine yields a charged choline-like moiety similar to that of PCs. Due to their polarity and relatively cylindrical shape, PCs spontaneously form bilayers, whereas the cone shape of PEs (nonmethylated equivalents of PC) causes them to assemble into inverted hexagonal phases. Perhaps, the additional three methyl groups in the head group of TMO also give it a more cylindrical shape and greater polarity than nonmodified ornithine lipids and thus result in greater bilayer stability. The ombrotrophic wetlands from which these planctomycetes were isolated are acidic and nutrient-poor ecosystems, and all four species in which the TMO lipid were observed are moderately acidophilic (19, 21, 22). Increased membrane stability provided by a polar quaternary amine in lipid head groups would be beneficial to these organisms in their native environment. Furthermore, because these ecosystems are nutrient limited, the synthesis of TMO lipids could provide membrane stability without relying on limited phosphorus. It has been shown that marine microbes under phosphorus-limited conditions switch from producing phosphorus-containing membrane lipids, such as PCs and PGs, to non-phosphorus-containing lipids, such as betaines and sulfoquinovosyl diacylglycerols (SQDGs), to maintain growth and survival (59). We hypothesize that the increased polarity and possible cylindrical shape of the trimethylornithine head group provide membrane stability without using scarce phosphorus and are thus adaptations to the acidic, nutrient-poor conditions of *Sphagnum*-dominated European north Russian wetlands.

The distributions of core lipid chains among MMO, DMO, and TMO lipids in *T. sphagniphila* are identical among the three lipid classes (Table 2). There are also many similarities in core lipid distribution among MMO, DMO, and TMO lipids within the extracts of *S. rosea*, *S. acidiphila*, and *Gemmata*-like strain SP5. The similar fatty acid distributions among the three lipid classes within each species suggest a biosynthetic link between the classes. This sequence of lipids with increasing methylation is not unprecedented in membrane lipids. One of the pathways for biosynthesis of PC involves sequential methylation of PE by the enzyme phosphatidylethanolamine *N*-methyltransferase, producing MMPE and DMPE as intermediates (60–62). A similar methylation process of the ornithine lipid head group may be involved in the biosynthesis of methylornithine lipids.

Pyrosequencing of bacterial 16S rRNA gene fragments was performed by Kulichevskaya et al. (22) for the peat sample

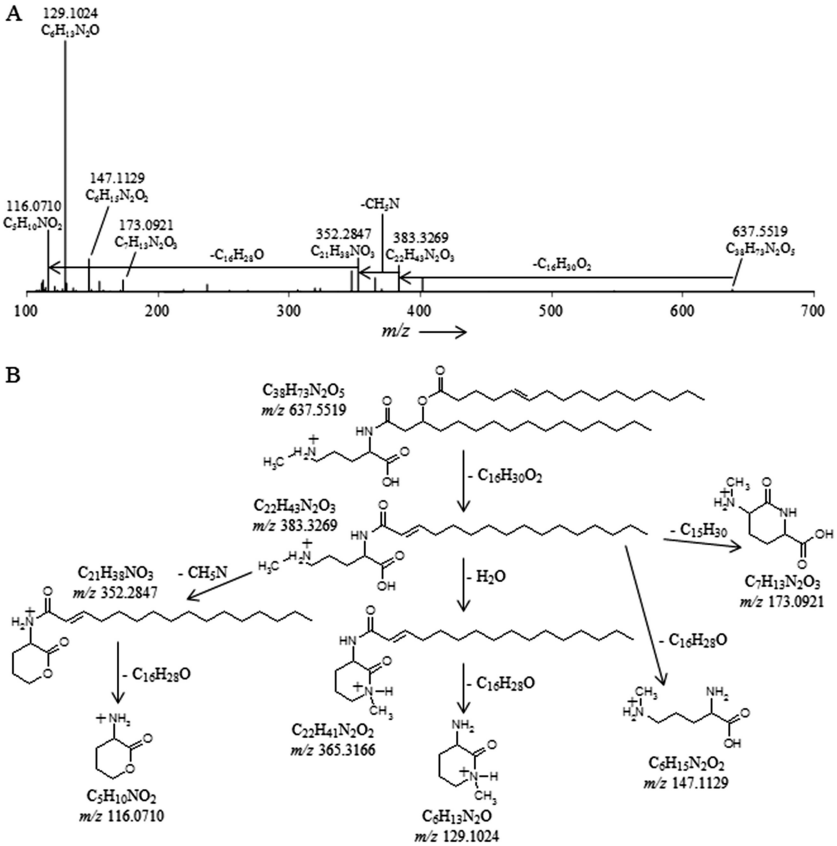

FIG 5 (A) High-resolution accurate-mass quadrupole OT/MS^2 mass spectrum of *T. sphagniphila* lipid extract group I monomethylornithine *m/z* 637.5519. The chemical formulas represent neutral losses and products after MS^2 fragmentation. (B) Proposed gas phase fragmentation pathway of monomethylornithine *m/z* 637.5519.

from which *T. sphagniphila* was originally isolated in order to assess the importance of this species to the *Planctomycetes* community. The study revealed that *T. sphagniphila* accounted for 10% of the planctomycete-related reads obtained from the peat sample, suggesting that *T. sphagniphila* is a typical representative of *Planctomycetes* in peat bogs (22). *Singulisphaera*-like planctomycetes were also abundant in the peat sample. However, the majority (61%) of all planctomycete-related 16S rRNA gene sequences retrieved from the sample could not be assigned to taxonomically described organisms, leaving open the possibility that other species at this location produce TMO lipids, as well. *Planctomycetes* have been observed to account for up to 14% of total bacterial cells in the upper, oxic peat layers of acidic northern wetlands and were mostly represented by members of the *Isosphaera-Singulisphaera* group (17). This suggests that the TMOs may be an important membrane constituent in the *Planctomycetes* community in peat bogs and may serve as an important environmental adaptation to the group's function as slow-acting decomposers of plant-derived organic matter. Further research is needed to investigate the specific functions of these lipids; the mono-, di-, and trimethylated ornithine lipid biosynthetic pathway; and the importance of methylornithine lipids in ombrotrophic environments.

REFERENCES

1. **Kivinen E, Pakarinen P.** 1981. Geographical distribution of peat resources and major peatland complex types in the world. Ann. Acad. Sci. Fenn. **132:**1–28.
2. **Gorham E.** 1991. Northern peatlands: role in carbon cycle and probable responses to climate warming. Ecol. Appl. **1:**182–195.
3. **Bain CG, Bonn A, Stoneman R, Chapman S, Coupar A, Evans M, Gearey B, Howat M, Joosten H, Keenleyside C, Labadz J, Lindsay R, Littlewood N, Lunt P, Miller CJ, Moxey A, Orr H, Reed M, Smith P, Swales V, Thompson DBA, Thompson PS, Van de Noort R, Wilson JD, Worrall F.** 2011. IUCN UK Commission of Inquiry on Peatlands. IUCN UK Peatland Programme, Edinburgh, United Kingdom.
4. **Gajewski K, Viau A, Sawada M, Atkinson D, Wilson S.** 2001. *Sphagnum* peatland distribution in North America and Eurasia during the past 21,000 years. Global Biogeochem. Cycles **15:**297–310.
5. **Clymo RS.** 1965. Experiments on breakdown of *Sphagnum* in two bogs. J. Ecol. **53:**747–758.
6. **Coulson JC, Butterfield J.** 1978. An investigation of the biotic factors determining the rates of plant decomposition on blanket bog. J. Ecol. **66:**631–650.
7. **Johnson LC, Damman AWH.** 1993. Decay and its regulation in *Sphagnum* peatlands. Adv. Bryol. **5:**249–296.
8. **Verhoeven JTA, Liefveld WM.** 1997. The ecological significance of organochemical compounds in *Sphagnum*. Acta Bot. Neerl. **46:**117–130.
9. **Aerts R, Wallén B, Malmer N, de Caluwe H.** 2001. Nutritional constraints on Sphagnum—growth and potential decay in northern peatlands. J. Ecol. **89:**292–299.
10. **Moore PD, Bellamy DJ.** 1974. Peatlands. Elek Science, London, United Kingdom.
11. **Clymo RS.** 1984. The limits to peat bog growth. Philos. Trans. R. Soc. Lond. B Biol. Sci. **303:**605–654.
12. **Botch MS, Kobak KI, Vinson TS, Kolchugina TP.** 1995. Carbon pools and accumulation in peatlands of the former Soviet Union. Global Biogeochem. Cycles **9:**37–46.
13. **Dedysh SN, Pankratov TA, Belova SE, Kulichevskaya IS, Liesack W.** 2006. Phylogenetic analysis and in situ identification of *Bacteria* commu-

nity composition in an acidic *Sphagnum* peat bog. Appl. Environ. Microbiol. **72:**2110–2117.
14. **Kulichevskaya IS, Belova SE, Kevbrin VV, Dedysh SN, Zavarzin GA.** 2007. Analysis of the bacterial community developing in the course of the *Sphagnum* moss decomposition. Microbiologiia **76:**702–710.
15. **Pankratov TA, Ivanova AO, Dedysh SN, Liesack W.** 2011. Bacterial populations and environmental factors controlling cellulose degradation in an acidic *Sphagnum* peat. Environ. Microbiol. **13:**1800–1814.
16. **Kulichevskaia IS, Pankratov TA, Dedysh SN.** 2006. Detection of representatives of the *Planctomycetes* in *Sphagnum* peat bogs by molecular and cultivation approaches. Microbiology **75:**389–396.
17. **Ivanova AO, Dedysh SN.** 2012. Abundance, diversity, and depth distribution of *Planctomycetes* in acidic northern wetlands. Front. Microbiol. **3:**5.
18. **Kulichevskaya IS, Ivanova AO, Belova SE, Baulina OI, Bodelier PLE, Rijpstra WIC, Sinninghe Damsté JS, Zavarzin GA, Dedysh SN.** 2007. Schlesneria paludicola gen. nov., sp. nov., the first acidophilic member of the order *Planctomycetes* from *Sphagnum*-dominated boreal wetlands. Int. J. Syst. Evol. Microbiol. **57:**2680–2687.
19. **Kulichevskaya IS, Ivanova AO, Baulina OI, Bodelier PLE, Sinninghe Damsté JS, Dedysh SN.** 2008. *Singulisphaera acidiphila* gen. nov., sp. nov., a non-filamentous, *Isosphaera*-like planctomycete from acidic northern wetlands. Int. J. Syst. Evol. Microbiol. **58:**1186–1193.
20. **Kulichevskaya IS, Baulina OI, Bodelier PLE, Rijpstra WIC, Sinninghe Damsté JS, Dedysh SN.** 2009. *Zavarzinella formosa* gen. nov., sp. nov., a novel stalked, *Gemmata*-like planctomycete from a Siberian peat bog. Int. J. Syst. Evol. Microbiol. **59:**357–364.
21. **Kulichevskaya IS, Detkova EN, Bodelier PLE, Rijpstra WIC, Sinninghe Damsté JS, Dedysh SN.** 2012. *Singulisphaera rosea*, sp. nov., a planctomycete from *Sphagnum* peat, and emended description of the genus *Singulisphaera*. Int. J. Syst. Evol. Microbiol. **62:**118–123.
22. **Kulichevskaya IS, Serkebaeva YM, Kim Y, Rijpstra WIC, Sinninghe Damsté JS, Liesack W, Dedysh SN.** 2012. Telmatocola sphagniphila gen. nov., sp. nov., a novel dendriform planctomycete from northern wetlands. Front. Microbiol. **3:**146.
23. **St-Hilaire F, Wu J, Roulet NT, Folking S, Lafleur PM, Humphreys ER, Arora V.** 2010. McGill wetland model: evaluation of a peatland carbon simulator developed for global assessments. Biogeoscience **7:**3517–3530.
24. **Wu J, Roulet NT, Nilsson M, Lafleur P, Humphreys E.** 2012. Simulating the carbon cycling of northern peatlands using a land surface scheme coupled to a wetland carbon model. Atmos. Ocean **50:**487–506.
25. **Kirschbaum MUF.** 1995. The temperature dependence of soil organic matter decomposition, and the effect of global warming on soil organic C storage. Soil Biol. Biochem. **27:**753–760.
26. **Biasi C, Rusalimova O, Meyer H, Kaiser C, Wanek W, Barsukov P, Junger H, Richter A.** 2005. Temperature-dependent shift from labile to recalcitrant carbon sources of arctic heterotrophs. Rapid Commun. Mass Spectrom. **19:**1401–1408.
27. **Dorrepaal E, Toet S, van Logtestijn RSP, Swart E, van de Weg MJ, Callaghan TV, Aerts R.** 2009. Carbon respiration from subsurface peat accelerated by climate warming in the subarctic. Nature **460:**616–620.
28. **Sturt HF, Summons RE, Smith K, Elvert M, Hinrichs KU.** 2004. Intact polar membrane lipids in prokaryotes and sediments deciphered by high-performance liquid chromatography/electrospray ionization multistage mass spectrometry—new biomarkers for biogeochemistry and microbial ecology. Rapid Commun. Mass Spectrom. **18:**617–628.
29. **Schubotz F, Wakeham SG, Lipp JS, Fredericks HF, Hinrichs KU.** 2009. Detection of microbial biomass by intact polar membrane lipid analysis in the water column and surface sediments of the Black Sea. Environ. Microbiol. **11:**2720–2734.
30. **Staley JT, Fuerst JA, Giovannoni S, Schlesner H.** 1992. The order *Planctomycetales* and the genera *Planctomyces*, *Pirellula*, *Gemmata* and *Isosphaera*, p 3710–3731. *In* Balows A, Truper H, Dworkin M, Harder W, Schleifer KH (ed), The prokaryotes: a handbook on the biology of bacteria: ecophysiology, isolation, identification, applications, 2nd ed. Springer, NewYork, NY.
31. **Rütters H, Sass H, Cypionka H, Rullkötter J.** 2002. Phospholipid analysis as a tool to study complex microbial communities in marine sediments. J. Microbiol. Methods **48:**149–160.
32. **Sinninghe Damsté JS, Rijpstra WIC, Hopmans EC, Weijers JWH, Foesel BU, Overmann J, Dedysh SN.** 2011. 13,16-Dimethyl octacosanedioic acid (iso-diabolic acid), a common membrane-spanning lipid of *Acidobacteria* subdivisions 1 and 3. Appl. Environ. Microbiol. **77:**4147–4154.
33. **Sinninghe Damsté JS, Rijpstra WIC, Schouten S, Fuerst JA, Jetten MSM, Strous M.** 2004. The occurrence of hopanoids in planctomycetes: implications for the sedimentary biomarker record. Org. Geochem. **35:**561–566.
34. **Boumann HA, Longo ML, Stroeve P, Poolman B, Hopmans EC, Stuart MCA, Sinninghe Damsté JS, Schouten S.** 2009. Biophysical properties of membrane lipids of anammox bacteria. I. Ladderane phospholipids form highly organized fluid membranes. Biochim. Biophys. Acta **1788:**1444–1451.
35. **Smittenberg RH, Hopmans EC, Schouten S, Sinninghe Damsté JS.** 2002. Rapid isolation of biomarkers for compound specific radiocarbon dating using high performance liquid chromatography and flow injection analysis-atmospheric pressure chemical ionisation mass spectrometry. J. Chromatogr. A **978:**129–140.
36. **Zhang X, Ferguson-Miller SM, Reid GE.** 2009. Characterization of ornithine and glutamine lipids extracted from cell membranes of *Rhodobacter sphaeroides*. J. Am. Soc. Mass. Spectrom. **20:**198–212.
37. **Okuyama H, Monde K.** 1996. Identification of an ornithine-containing lipid from *Cytophaga johnsonae* Stanier strain C21 by ^{1}H-NMR. Chem. Phys. Lipids **83:**169–173.
38. **Linscheid M, Diehl BWK, Overmohle M, Riedl I, Heinz E.** 1997. Membrane lipids of *Rhodopseudomonas viridis*. Biochim. Biophys. Acta **1347:**151–163.
39. **Hamilton JA, Morrisett JD.** 1986. Nuclear magnetic resonance studies of lipoproteins. Methods Enzymol. **128:**472–515.
40. **Gunstone FD.** 1994. High resolution ^{13}C NMR. A technique for the study of lipid structure and composition. Prog. Lipid Res. **33:**19–28.
41. **Tugnoli V, Bottura G, Fini G, Reggiani A, Tinti A, Trinchero A, Tosi MR.** 2003. ^{1}H-NMR and ^{13}C-NMR lipid profiles of human renal tissues. Biopolymers **72:**86–95.
42. **Lopez-Lara IM, Sohlenkamp C, Geiger O.** 2003. Membrane lipids in plant-associated bacteria: their biosynthesis and possible functions. Mol. Plant Microbe Interact. **16:**567–579.
43. **Geiger O, Gonzalez-Silva N, Lopez-Lara IM, Sohlenkamp C.** 2010. Amino acid-containing membrane lipids in bacteria. Prog. Lipid Res. **49:**46–60.
44. **Vences-Guzman MA, Geiger O, Sohlenkamp C.** 2012. Ornithine lipids and their structural modifications from A to E and beyond. FEMS Microbiol. Lett. **335:**1–10.
45. **Freer E, Moreno E, Moriyon I, Pizarro-Cerda J, Weintraub A, Gorvel JP.** 1996. *Brucella-Salmonella* lipopolysaccharide chimeras are less permeable to hydrophobic probes and more sensitive to cationic peptides and EDTA than are their native *Brucella* sp. counterparts. J. Bacteriol. **178:**5867–5876.
46. **Weissenmayer B, Gao JL, Lopez-Lara IM, Geiger O.** 2002. Identification of a gene required for the biosynthesis of ornithine-derived lipids. Mol. Microbiol. **45:**721–733.
47. **Gao JL, Weissenmayer B, Taylor AM, Thomas-Oates J, Lopez-Lara IM, Geiger O.** 2004. Identification of a gene required for the formation of lyso-ornithine lipid, an intermediate in the biosynthesis of ornithine-containing lipids. Mol. Microbiol. **53:**1757–1770.
48. **Taylor CJ, Anderson AJ, Wilkinson SG.** 1998. Phenotypic variation of lipid composition in *Burkholderia cepacia*: a response to increased growth temperature is a greater content of 2-hydroxy acids in phosphatidylethanolamine and ornithine amide lipid. Microbiology **144:**1737–1745.
49. **Rojas-Jimenez K, Sohlenkamp C, Geiger O, Martinez-Romero E, Werner D, Vinuesa P.** 2005. A CIC chloride channel homolog and ornithine-containing membrane lipids of Rhizobium tropici CIAT899 are involved in symbiotic efficiency and acid tolerance. Mol. Plant Microbe Interact. **18:**1175–1185.
50. **Vences-Guzman MA, Guan Z, Ormeno-Orillo E, Gonzalez-Silva N, Geiger O, Sohlenkamp C.** 2011. Hydroxylated ornithine lipids increase stress tolerance in *Rhizobium tropici* CIAT899. Mol. Microbiol. **79:**1496–1514.
51. **Kawazoe R, Okuyama H, Reichardt W, Sasaki S.** 1991. Phospholipids and a novel glycine containing lipoamino acid in *Cytophaga johnsonae* Stainier strain C21. J. Bacteriol. **173:**5470–5475.
52. **Batrakov SG, Nikitin DI, Mosezhnyi AE, Ruzhitsky AO.** 1999. A glycine containing phosphorus-free lipoaminoacid from the gram-negative marine bacterium *Cyclobacterium marinus* WH. Chem. Phys. Lipids **99:**139–143.

53. **Tahara Y, Yamada Y, Kondo K.** 1976. A new lysine-containing lipid isolated from *Agrobacterium tumefaciens*. Agric. Biol. Chem. **40:**1449–1450.
54. **Tahara Y, Kameda M, Yamada Y, Kondo K.** 1976. A new lipid; the ornithine and taurine-containing "cerilipin". Agric. Biol. Chem. **40:**243–244.
55. **Brown JL, Ross T, McMeekin TA, Nichols PD.** 1997. Acidic habituation of *Escherichia coli* and the potential role of cyclopropane fatty acids in low pH tolerance. Int. J. Food Microbiol. **37:**163–173.
56. **Bearson S, Bearson B, Foster JW.** 1997. Acidic stress responses in enterobacteria—minireview. FEMS Microbiol. Lett. **147:**173–180.
57. **Álvarez-Ordóñez A, Fernández A, López M, Bernardo A.** 2009. Relationship between membrane fatty acid composition and heat resistance of acid and cold stressed *Salmonella senftenberg* CECT 4348. Food Microbiol. **26:**347–353.
58. **Gianotti A, Iucci L, Guerzoni ME, Lanciotti R.** 2009. Effect of acidic conditions on fatty acid composition and membrane fluidity of *Escherichia coli* strains isolated from Crescenza cheese. Ann. Microbiol. **59:**603–610.
59. **Van Mooy BAS, Fredericks HF, Pedler BE, Dyhrman ST, Karl DM, Koblizek M, Lomas MW, Mincer TJ, Moore LR, Moutin T, Rappé MS, Webb EA.** 2009. Phytoplankton in the ocean use non-phosphorus lipids in response to phosphorus scarcity. Nature **458:**69–72.
60. **Bremer J, Greenberg DM.** 1961. Methyl transferring enzyme system of microsomes in biosynthesis of lecithin (phosphatidylcholine). Biochim. Biophys. Acta **46:**205–216.
61. **Yamashita S, Oshima A, Nikawa J, Hosaka K.** 1982. Regulation of the phosphatidylethanolamine methylation pathway in *Saccharomyces cerevisiae*. Eur. J. Biochem. **128:**589–595.
62. **Gaynor PM, Gill T, Toutenhoofd S, Summers EF, McGraw P, Homann MJ, Henry SA, Carman GM.** 1991. Regulation of phosphatidylethanolamine methyltransferase and phospholipid methyltransferase by phospholipid precursors in *Saccharomyces cerevisiae*. Biochim. Biophys. Acta **1090:**326–332.
63. **Kostiainen R, Tuominen J, Luukanen L, Taskinen J, Green BN.** 1997. Accurate mass measurements of some glucuronide derivatives by electrospray low resolution quadrupole mass spectrometry. Rapid Commun. Mass Spectrom. **11:**283–285.
64. **Sakayanagi M, Yamada Y, Sakabe C, Watanabe K, Harigaya Y.** 2006. Identification of inorganic anions by gas chromatography/mass spectrometry. Forensic Sci. Int. **157:**134–143.
65. **Calza P, Medana C, Padovano E, Dal Bello F, Baiocchi C.** 2012. Identification of the unknown transformation products derived from lincomycin using LC-HRMS technique. J. Mass Spectrom. **47:**751–759.